Si nanoparticles embedded in pseudo binaries alloys with Al_2O_3

P Vitanov[1], A Harizanova[1], T Ivanova[1] and A Ulyashin[2]

[1]Central Laboratory of Solar Energy and New Energy Sources, Bulgarian Academy of Sciences, Blvd. Tzarigradsko chaussee 72, Sofia, Bulgaria
[2]SINTEF Materials and Chemistry, Metallurgy Department, Forskningsveien 1, Blindern, NO-0314 Oslo, Norway

E-mail: vitanov@phys.bas.bg

Abstract. The present paper reports the incorporation of Si nanoparticles (NPs) in $(Al_2O_3)_x$ $(B_2O_3)_{1-x}$ films. A new approach for involving Si NPs (20 nm) p^+ doped into sol solution was used. After spin coating deposition and additional annealing at 850°C, $(Al_2O_3)_x$ $(B_2O_3)_{1-x}$ films with Si NPs have been obtained with thickness of 75 and 120 nm. The $(Al_2O_3)_x$ $(B_2O_3)_{1-x}$ films were deposited on p-type and n-type Si wafers. The optical study reveals that Si NPs embedded in $(Al_2O_3)_x(B_2O_3)_{1-x}$ leads to higher absorption in the visible spectral range compared to dielectric layer without nanoparticles. AFM studies show that the incorporated Si nanoparticles into the dielectric layer have probably a uniform distribution on film surface. This conclusion is confirmed by SEM observation. The current - voltage (I-V) characteristics of a structure $(Al_2O_3)_x(B_2O_3)_{1-x}$ layer with Si NPs on p- type Si shows an ohmic type of conductivity. The sheet resistance is 480 Ohm/sq respectively, when the same layer is deposited on quartz substrate. This work presents a new technological approach for integration of Si NPs in dielectric matrix of $(Al_2O_3)_x$ $(B_2O_3)_{1-x}$. The results can find applications for formation of ultra thin emitter for photodiodes and Si solar cells.

1. Introduction

Materials with nano particles (NPs) form a new class of artificial materials with tuneable electronic properties controlled at the nanoscale and composed of close-packed granules varying in size from a few to hundreds of nanometers -often referred to as *nanocrystals*. Their properties discover a new route for potential novel electronic, optical, and optoelectronic applications.

Applications range from light-emitting devices to photovoltaic cells and biosensors. Among traditional methods of preparation of such materials, the most common are thermal evaporation and sputtering techniques. During those processes metallic and insulating components are simultaneously evaporated or sputtered onto a substrate. Diffusion of the metallic component leads to the formation of small metallic grains, usually 3–50 nm in diameter.

Another approach is Si nanocrystallites embedded in dielectric matrices. The Si NPs in oxide matrix exhibit unique electrical, optical, and optoelectronical properties [1-4]. Among different dielectric materials, silicon oxide is the most addressed as a host for Si NPs [4, 5]. During the last

[1] To whom any correspondence should be addressed.

decades, the properties of Si NPs-SiO_2 systems have been widely investigated. Several approaches have been used to form Si-NPs in amorphous and/or crystalline Al_2O_3. Most known methods are Si ion implantation [7, 8] and electron beam evaporation followed by subsequent high-temperature annealing as well as laser ablation [9].

The present paper reports the fabrication of Si NPs in $(Al_2O_3)_x (B_2O_3)_{1-x}$ films. A new approach for involving Si nanoparticles (20 nm) p^+ doped into sol solution was used. After spin coating deposition and additional annealing at 850°C, thin $(Al_2O_3)_x (B_2O_3)_{1-x}$ films with Si NPs have been obtained.

2. Experimental

The sol solution preparation for depositing $(Al_2O_3)_x(B_2O_3)_{1-x}$ films has been previously reported [10]. The used Si nanoparticles are p^+ doped and 20 nm sized, fabricated by SINTEF.

Suitable receipt for homogenization of Si NPs has been developed. Homogeneous, stable suspensions in sol solution were obtained by mixing the respective amount of nanoparticles with sol solution followed by ultrasonic treatment of the dispersion. Thin films with thickness of 75 and 120 nm were obtained by spin coating method on Si wafers or quartz substrates and substantial additional annealing at 850°C.

For comparison, $(Al_2O_3)_x(B_2O_3)_{1-x}$ films with and without Si NPs have been deposited.

Scanning Electron Microscopy (SEM), High Resolution Transmission Electron microscopy (HRTEM) and Atomic Force microscopy (AFM) were used to determine the morphology of layers. Optical properties were studied by using UV-VIS-NIR Shimadzu 3600 spectrophotometer as for the sol-gel films obtained on quartz substrates.

The electrical properties of the films have been studied by forming MIS structures. The aluminium oxide thin films were deposited on p-type Si wafers, FZ, with 3.6-5.4 Ω.cm resistivity and an orientation <100>. The mercury probe was used as metal contact.

3. Results and discussions

3.1. Optical characterization

Optical measurements of $(Al_2O_3)_x (B_2O_3)_{1-x}$ films with and without Si NPs were performed and the results are compared in figure 1.

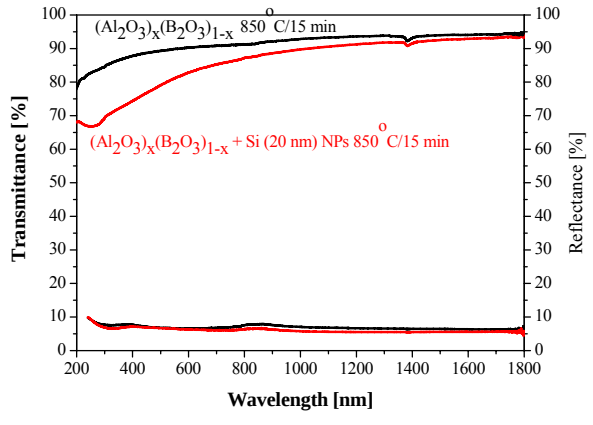

Figure 1. Spectral dependences of transmittance and the reflectance of layers, deposited on quartz substrates.

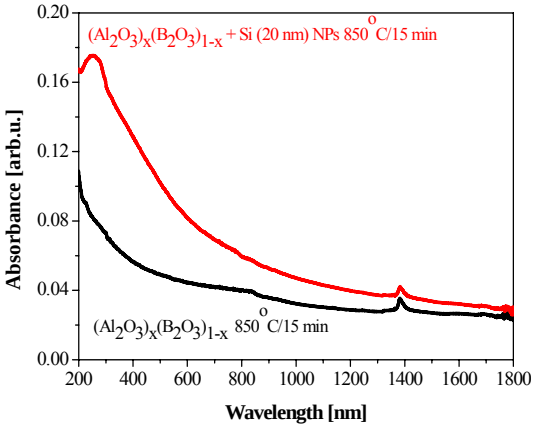

Figure 2. Optical absorbance of the thin layers with and without Si NP on quartz substrates.

The optical study reveals that the incorporation of Si NPs in $(Al_2O_3)_x(B_2O_3)_{1-x}$ leads to higher absorption in the visible spectral range up to 800 nm compared to dielectric layer without nanoparticles (figure 2) In the same time, no significant difference is observed in the mirror

reflectance recorded for $(Al_2O_3)_x(B_2O_3)_{1-x}$ layer without and with Si nanoparticles. The reflectance is below 10% in the whole spectral range.

3.2. Morphological studies

The surface morphology and microstructure of the layers were examined by AFM, TEM, SEM techniques.

The surface roughness of $(Al_2O_3)_x(B_2O_3)_{1-x}$ layer with Si nanoparticles (sample 3_3) and $(Al_2O_3)_x(B_2O_3)_{1-x}$ layer without Si nanoparticles (sample 6_3) is determined by AFM and the micrographs are shown in figures 3 and 4.

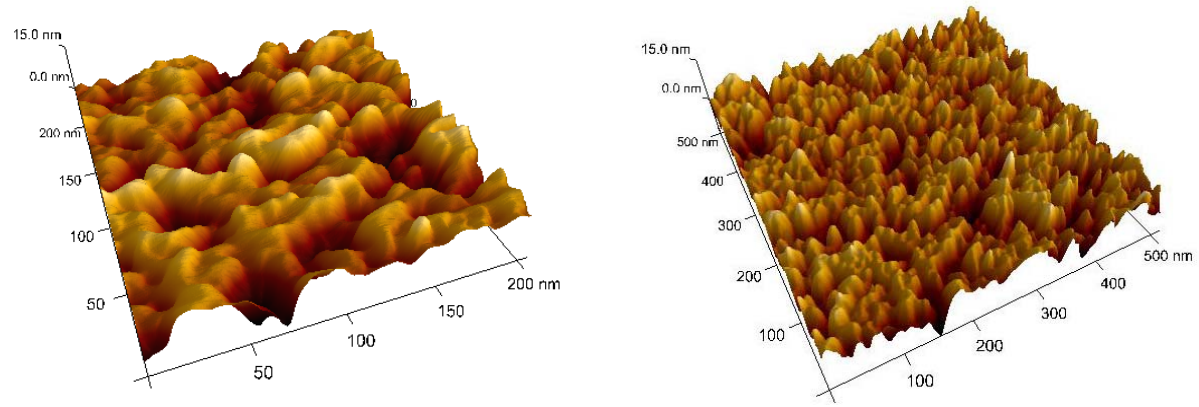

Figure 3. 3-D image of sample 3_3 $(Al_2O_3)_x(B_2O_3)_{1-x}$ layer (120 nm thick) with Si nanoparticles (20 nm).

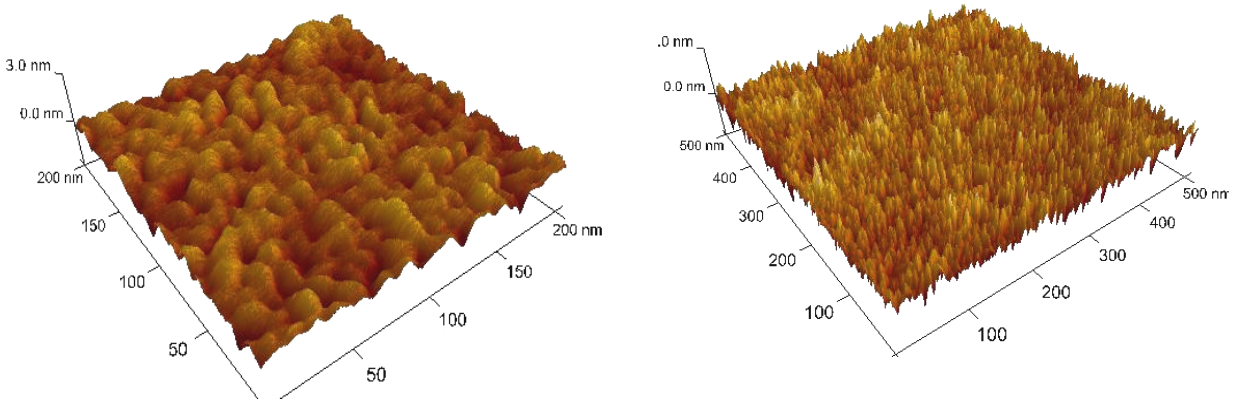

Figure 4. 3-D image of sample 6_3 with the same $(Al_2O_3)_x(B_2O_3)_{1-x}$ layer (120 nm) without Si nanoparticles.

On the surface of sample 3_3 can be clearly observed uniformly distributed granules in contrast to the surface of sample 6_3. RMS roughness for an area of 1 μm is R_q=0.345 nm for $(Al_2O_3)_x(B_2O_3)_{1-x}$ layer (120 nm) without Si NPs. More information for the sizes of the granules can be obtained from figure 5 and figure 6.

The surface of sample 6_3 has the characteristic morphology of $(Al_2O_3)_x(B_2O_3)_{1-x}$ with deviation of 1.5 nm from the middle plane.

The conclusions that can be derived from the AFM studies are that the embedded Si nanoparticles into the dielectric layer have probably a uniform distribution on the film surface.

This conclusion is confirmed by the surface morphology analysis by the means of SEM revealing uniformly distributed grains with sizes of 20 nm as it can be seen from figure 7.

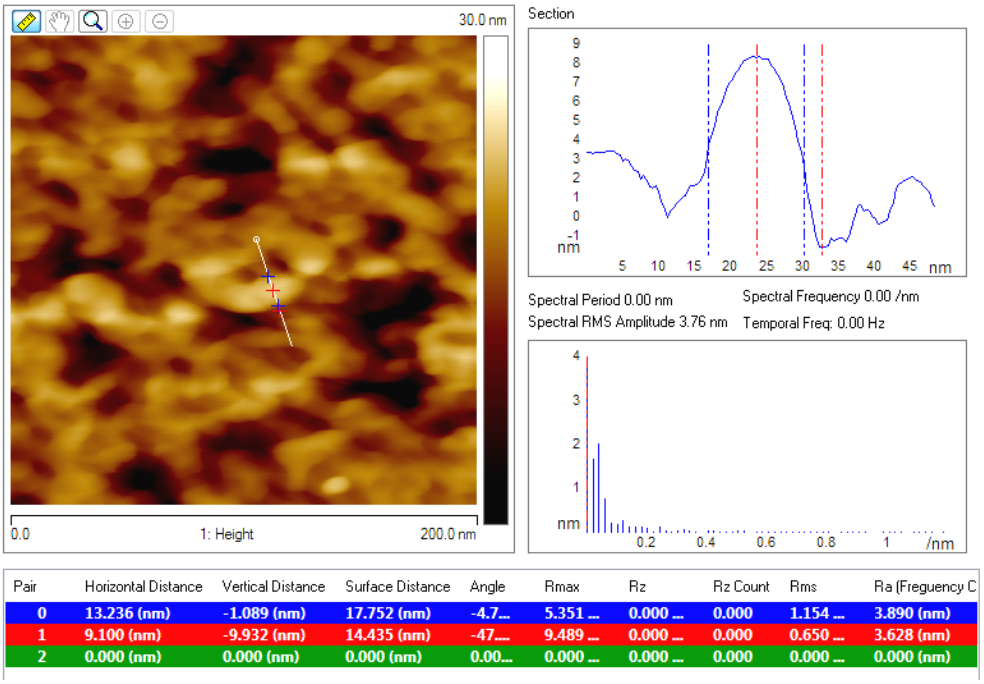

Pair	Horizontal Distance	Vertical Distance	Surface Distance	Angle	Rmax	Rz	Rz Count	Rms	Ra (Frequency C
0	13.236 (nm)	-1.089 (nm)	17.752 (nm)	-4.7...	5.351 ...	0.000 ...	0.000	1.154 ...	3.890 (nm)
1	9.100 (nm)	-9.932 (nm)	14.435 (nm)	-47....	9.489 ...	0.000 ...	0.000	0.650 ...	3.628 (nm)
2	0.000 (nm)	0.000 (nm)	0.000 (nm)	0.00...	0.000 ...	0.000 ...	0.000	0.000 ...	0.000 (nm)

Figure 5. AFM image of sample 3_3 $(Al_2O_3)_x(B_2O_3)_{1-x}$ layer (120 nm thick) with Si nanoparticles (20 nm). The size of the particle is: width 13 nm and height 9 nm.

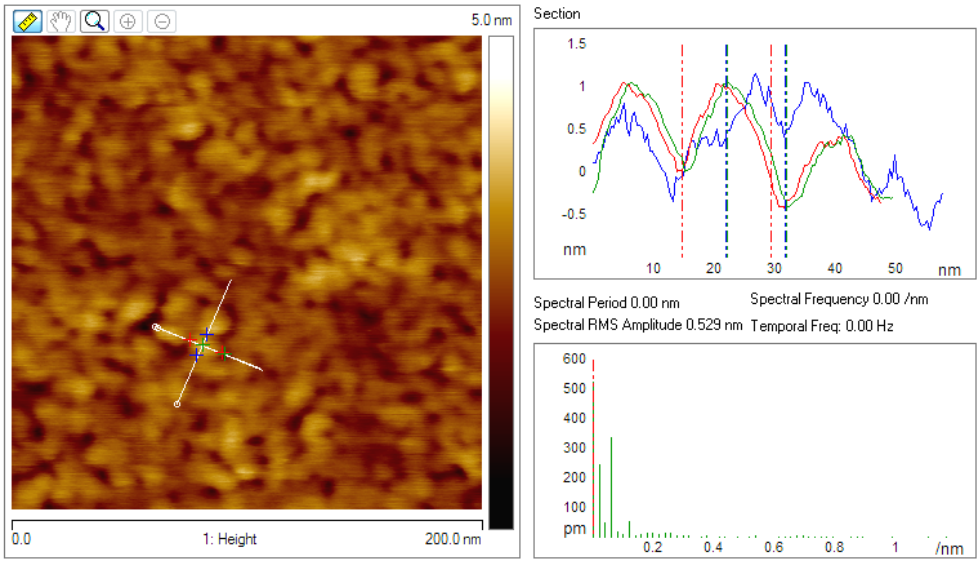

Pair	Horizontal Distance	Vertical Distance	Surface Distance	Angle	Rmax	Rz	Rz Count	Rms	Ra (Frequency C
0	9.786 (nm)	0.029 (nm)	10.097 (nm)	0.16...	0.735 ...	0.000 ...	0.000	0.191 ...	0.417 (nm)
1	14.745 (nm)	-0.109 (nm)	14.986 (nm)	-0.4...	1.134 ...	1.134 ...	2.000	0.319 ...	0.327 (nm)
2	9.690 (nm)	-1.465 (nm)	9.844 (nm)	-8.5...	1.304 ...	0.000 ...	0.000	0.392 ...	0.387 (nm)

Figure 6. AFM image of sample 6_3 $(Al_2O_3)_x(B_2O_3)_{1-x}$ layer without Si NPs.

The results from TEM observation on $(Al_2O_3)_x(B_2O_3)_{1-x}$ layer embedded with Si NPs are presented on figure 8. On the left side, the Si substrate is visible as highly periodic arranged atoms. Inside the dielectric, Si NPs with random crystal orientation are visible. Their size varies between 5 and 8 nm.

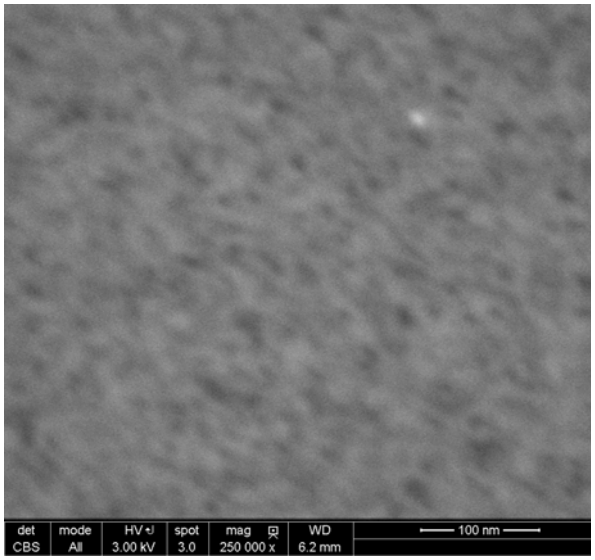

Figure 7. SEM micrograph of the dielectric surface embedded with Si NPs.

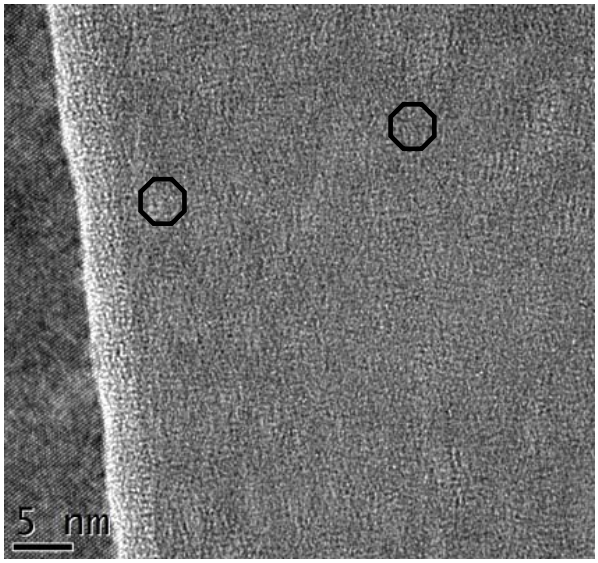

Figure 8. TEM micrograph of the dielectric surface embedded with Si NPs.

3.3. Electrical properties

The sheet resistance of the layer with Si NPs is 480 Ω/□, when the layer is deposited on quartz substrate at the same conditions. The electrical properties of the films have been studied by forming MIS structures. The aluminium oxide thin film with Si NPs was deposited on p-type Si wafers, FZ, with 3.6-5.4 Ω.cm resistivity and an orientation <100>. The mercury probe was used as metal contact.

The electrical measurements of this structure reveal that it has electrical conductivity towards Si substrate (figure 9). The I-V characteristic is similar to unipolar device and shows a symmetric behavior with respect to 0 V.

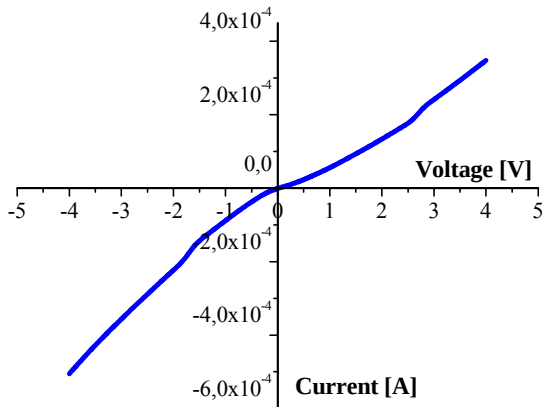

Figure 9. I-V characteristics of $(Al_2O_3)_x(B_2O_3)_{1-x}$ layer (120 nm thick) with Si NPs on p-type Si wafer.

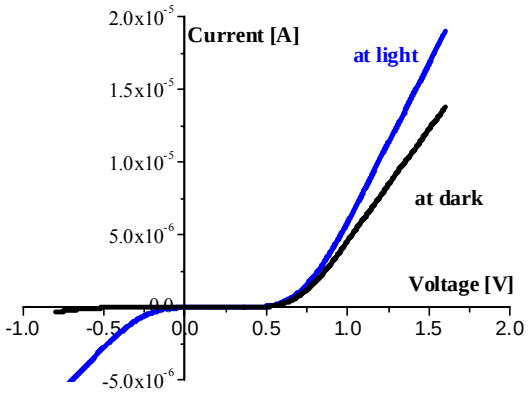

Figure 10. I-V curve of the $(Al_2O_3)_x(B_2O_3)_{1-x}$ layer with Si NPs on n- type Si wafer.

The electric behavior of $(Al_2O_3)_x(B_2O_3)_{1-x}$ layer without Si NPs (sample 6_3) is typical for dielectric. The breakdown voltage of the MIS structure is 19-20 V and the C-V curve shows negative fixed charge.

Figure 10 presents the I-V curve of a structure $(Al_2O_3)_x(B_2O_3)_{1-x}$ layer with Si NPs on n- type Si wafer. The current – voltage characteristic has a typical diode behavior of the p+/n junction. In contrast to the unipolar device (figure 9), this structure shows a clear rectifying diode-like behavior. Under reverse bias the current depends from light illumination. The difference in electrical behaviour between the unipolar device structure and the p/n junction structure proves the observed rectifying characteristic to be the result of the realized p-n junction and not the result of a Schottky contact [11].

4. Conclusions

An approach for integration of p^+ doped Si nanoparticles (20 nm) in $(Al_2O_3)_x(B_2O_3)_{1-x}$ matrix has been developed, using spin coating deposition of sol solution on Si substrates. Uniform distribution of Si nanoparticles has been observed on the film surface by AFM.

The films with embedded Si NPs reveal an electric conductivity towards Si substrate and the sheet resistance is 480 Ω/□, when it is deposited on quartz substrate. A p-n diode structure can been produced on n-type Si wafers using highly doped Si-NPs in combination with a high temperature sintering process.

References

[1] Dutta A, Kimura M, Honda Y, Otobe M, Itoh A and Oda S 1997 *Jpn. J. Appl. Phys.* 36 4038
[2] Choi H, Hwong S W, Kirn G, Shin H C, Kim Y and Kirn E K 1998 *Appl. Phys. Lett.* 73 3129
[3] Inokuma T, Wakayama Y, Muramoto T, Aoki R, Kurata Y and Hasegawa S 1998 *J. Appl. Phys.* 83 2228
[4] Seifarth D H, Gritzschel R, Markwitz A, Matz W, Nitzsche P and Rebohle L 1998 *Thin Solid Films* 330 202.
[5] Khomenkova L, Korsunska N, Yukhimchuk V, Jumaev B, Torchinska T, Vivas Hernandez, A Many A, Goldstein Y, Savir E and Jedrzejewski J 2003 *J. Lumin.* 102/103 705
[6] Chen X Y, Lu Y F, Tang L J, Wu Y H, Cho B J, Xu X J, Dong J R and Song W D 2005 *J. Appl. Phys.* 97 014913
[7] Mikhaylov A, Belov A, Kostyuk A, Zhavoronkov I, Korolev D, Nezhdanov A, Ershov A, Guseinov D, Gracheva T, Malygin N, Demidov E and Tetelbaum D 2012 *Phys Solid State* 54, 368
[8] Yerci S, Serincan U, Dogan I, Tokay S, Genisel M, Aydinli A and Turan R 2006 *J. Appl. Phys.* 100 074301
[9] Núñez-Sánchez S, Serna R, García López J, Petford-Long A, Tanase M, Kabius B 2009 *J. Appl. Phys.* 105 013118
[10] Vitanov P, Harizanova A, Ivanova T and Dimitrova T 2009 *Thin Solid Films* 517 6327
[11] Meseth M, Ziolkowski P, Schierning G, Theissmann R, Petermann N, Wiggers H, Bensona N, and Schmechel R 2012 *Scripta Materialia* 67 265